Supporting information

Inorganic Prodrug Tellurium Nanowire with Enhanced ROS Generation and GSH Depletion for Selective Cancer Therapy

Ying Wu[a], Tao Guo[a], Yuan Qiu[a], Yan Lin[a], Yunyan Yao[a], Weibin Lian[b], Lisen Lin[c], Jibin Song*[a], Huanghao Yang*[a]

[a.] *MOE Key Laboratory for Analytical Science of Food Safety and Biology, State Key Laboratory of Photocatalysis on Energy and Environment, College of Chemistry, Fuzhou University, Fuzhou 350116, P. R. China.*

[b.] *Department of Breast Surgery, Quanzhou First Hospital of Fujian, Medical University, Quanzhou 362000, P. R. China.*

[c.] *National Institute of Neurological Disorders and Stroke (NINDS), National Institutes of Health (NIH), Bethesda, Maryland 20892, United States.*

Corresponding Author

Jibin Song: jibinsong@fzu.edu.cn

Huanghao Yang: hhyang@fzu.edu.cn

Equipment: Transmission electron microscopy (TEM), high-resolution TEM (HRTEM), and X-ray spectroscopy (EDS) element analysis were captured on a Tecnai G2 F20 at an accelerating voltage of 200 kV. X-ray photoelectron (XPS) data were collected on a Thermo escalab 250Xi XPS spectrometer. X-ray diffraction spectrometry (XRD), were recorded on a Rigaku Ultima IV with Cu Ka radiation (1.5418 A). Ultraviolet-visible-near-infrared light (UV-Vis-NIR) absorption spectra was recorded using a SH-1000 Lab microplate reader (Corona Electric, Ibaraki, Japan). The tellurium concentration of the samples was determined by a XSERIES 2 ICP-MS. Inverted microscope picture was collecting by means of Nikon Ti-S (Tokyo, Japan). The confocal laser scanning microscopy (CLSM) imaging was obtained from Nikon A1 (Tokyo, Japan).

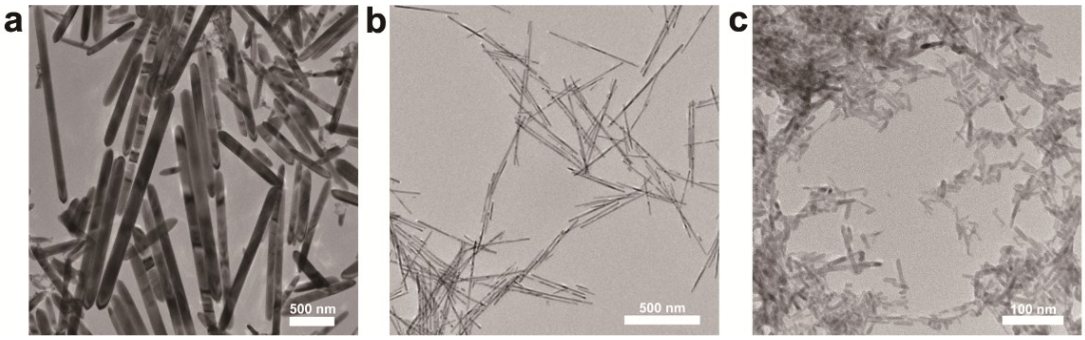

Fig. S1 Tellurium nanomaterials synthesized by different methods. (a) The product obtained by the reaction of hydrazine with sodium borohydride. (b) The product obtained by the reaction of hydrazine with sodium borohydride and BSA. (c) The product obtained by the reaction of hydrazine with sodium borohydride and dextran.

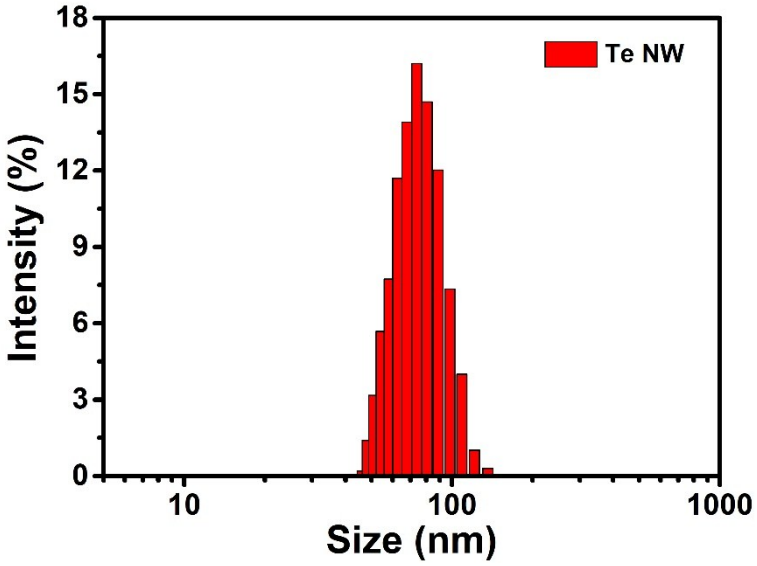

Fig. S2 The size of TeNW detected by DLS.

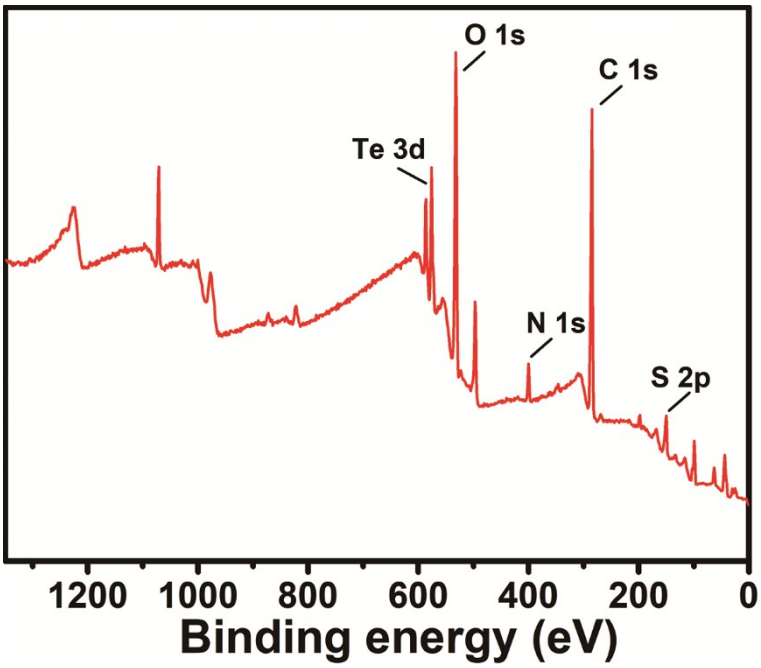

Fig. S3 The whole scan XPS spectra of TeNWs.

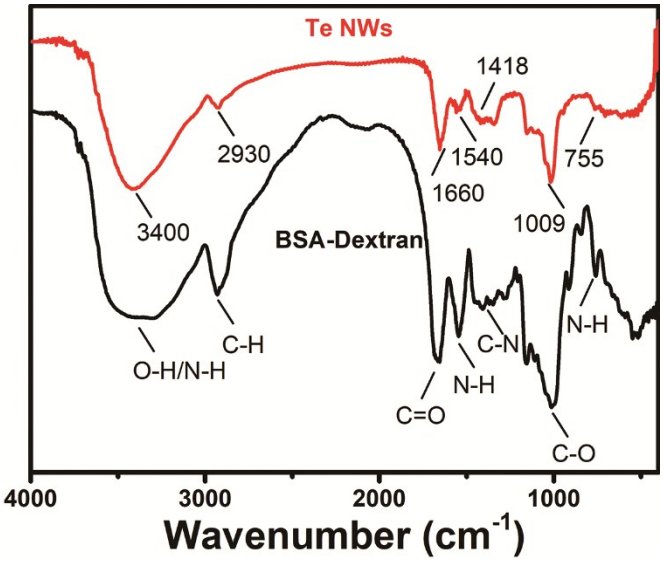

Fig. S4 FT-IR spectrum of TeNWs and BSA-dextran conjugates.

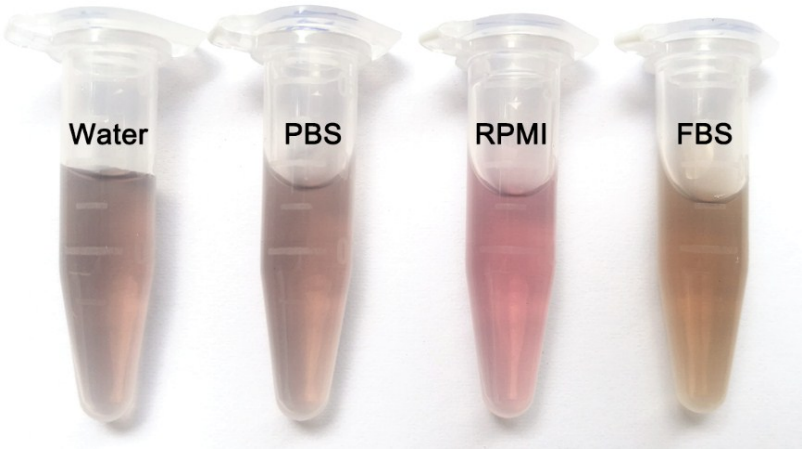

Fig. S5 Photographs of TeNWs dispersed in various medium (water, PBS, 1640 medium and FBS) after 30 days in 4 ℃.

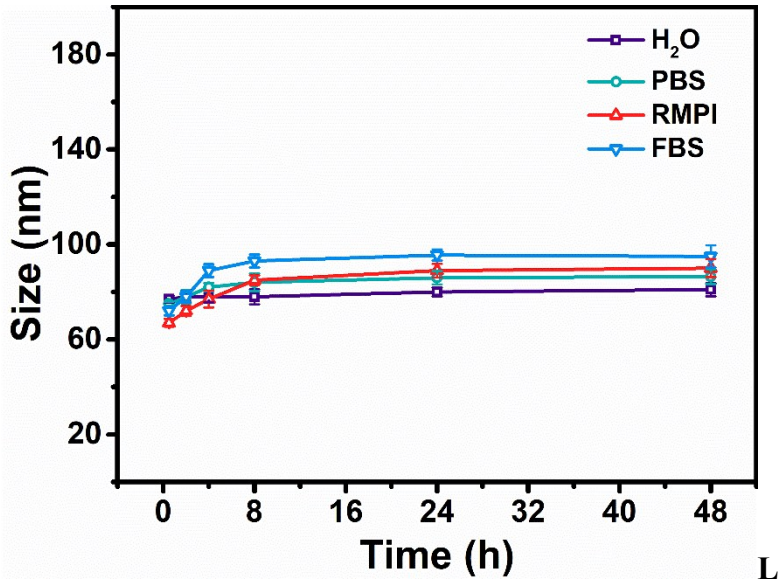

Fig. S6 Changes in the particle size of TeNW in H_2O, PBS, RMPI and FBS.

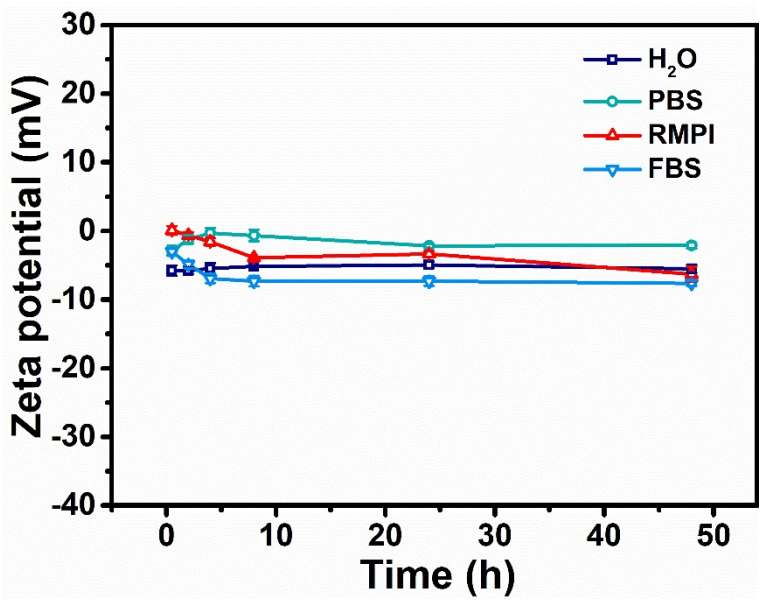

Fig. S7 Diagram of TeNW zeta potential charge over time in different kind of solutions.

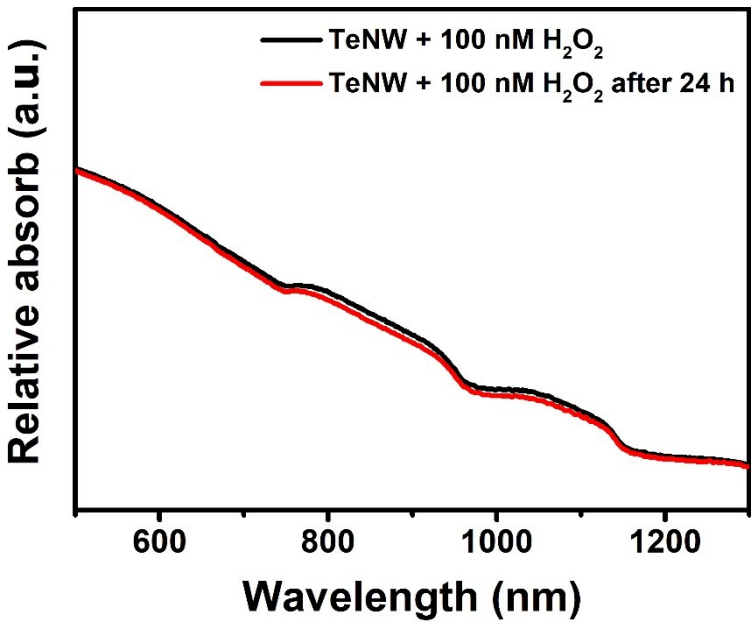

Fig. S8 UV/Vis absorption spectra of TeNW treated with H_2O_2 (100 nM)**.**

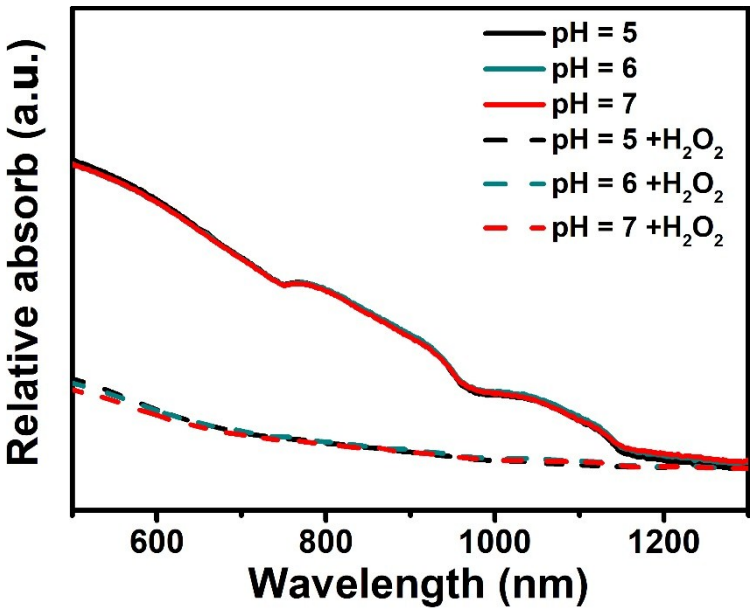

Fig. S9 TeNW in the same H_2O_2 concentration (100 μM) in the pH range of human body.

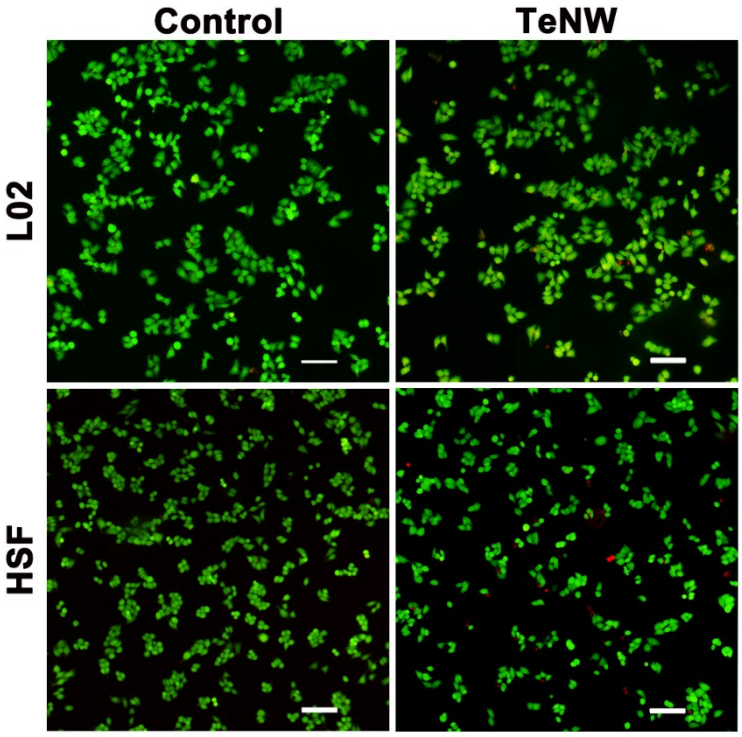

Fig. S10 Detection of normal cell activity by double staining of calcein-AM and PI.

The experimental group was treated with TeNW (40 μg/ml). scale bar: 100 μm.

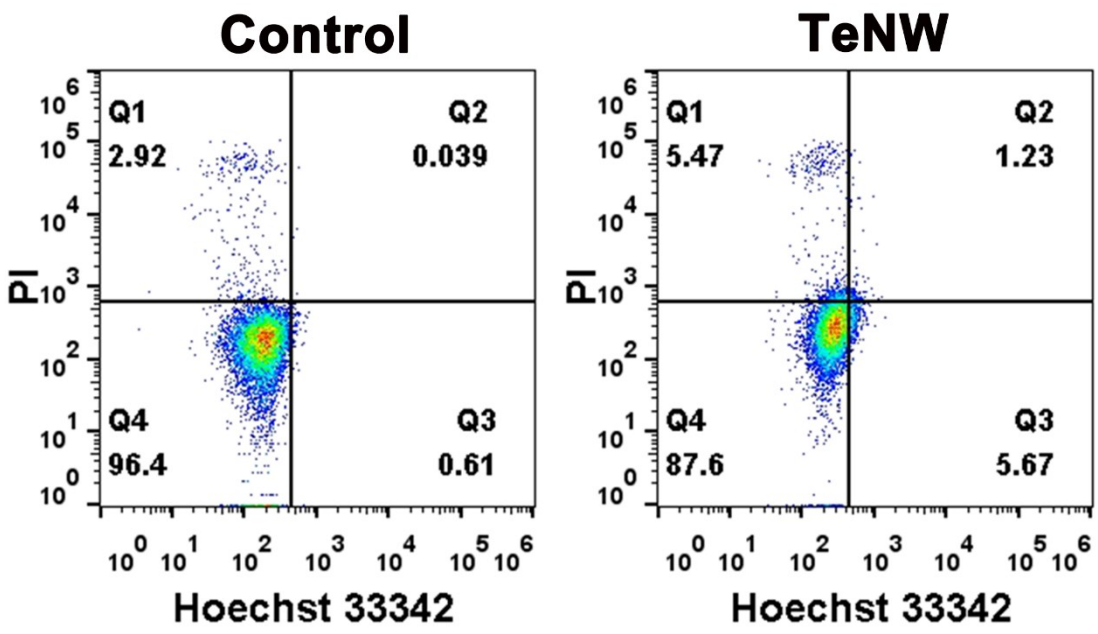

Fig S11 Diagram of Hoechest 33342/PI flow cytometry of MCF-7 cells after treatment with TeNW for 24 h. (Q1 represent the dead cells; Q2 + Q3 represent apoptotic cells; Q4 show viable cells).

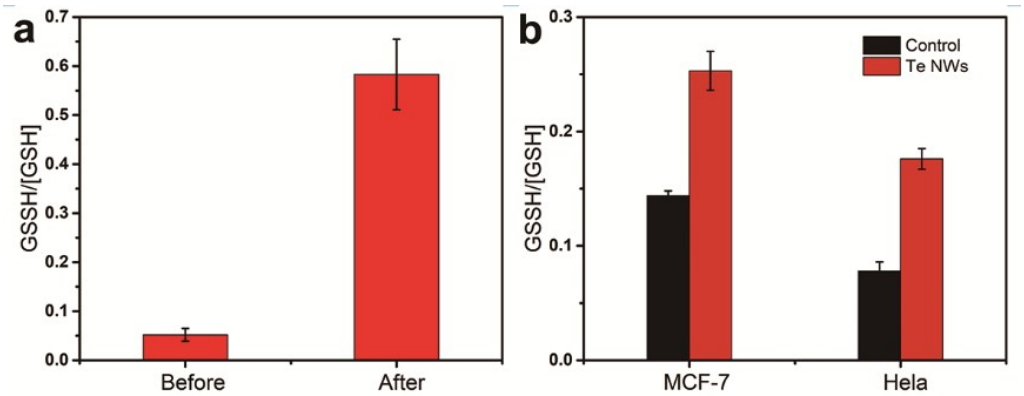

Fig. S12 (a) Ratio histogram of GSSH/[GSH] after H_6TeO_6 and GSH react for 12 h in vitro. (b) Histogram of the ratio of GSSH/GSH intracellular after TeNWs (24 μg/mL) incubated with MCF-7 and Hela cell for 24 h.

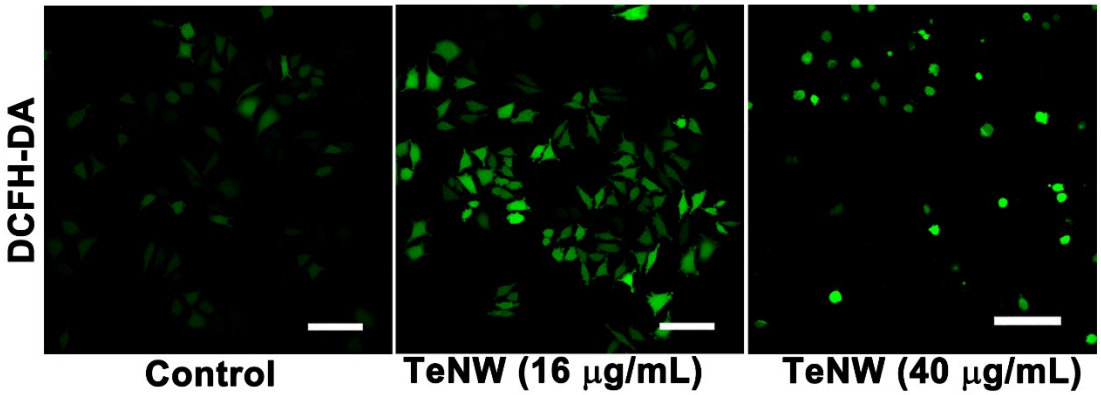

Fig. S13 Confocal fluorescence microscope images of MCF-7 cells after different treatments for 24h. scale bar: 100 μm.

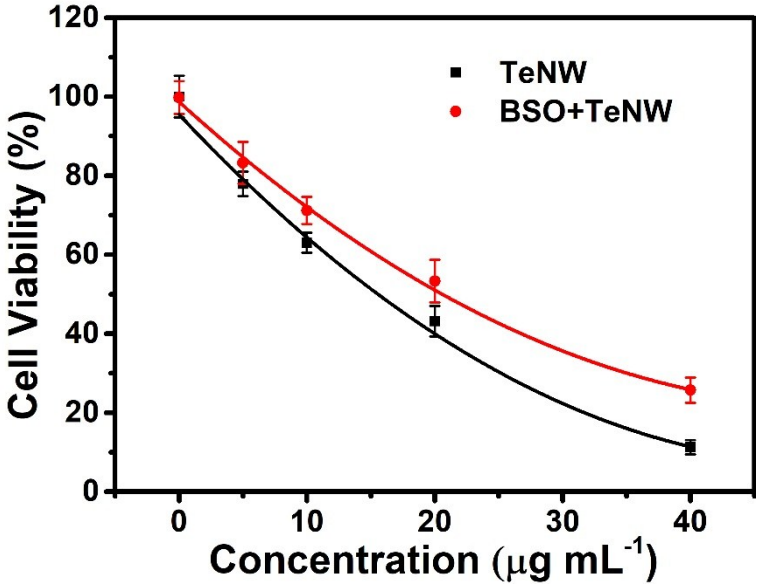

Fig. S14 The cell viability of MCF-7 cells treated with different concentrations of TeNW and GSH inhibitor BSO (5 mM) (red line) and TeNW only (black line) for 24 h.

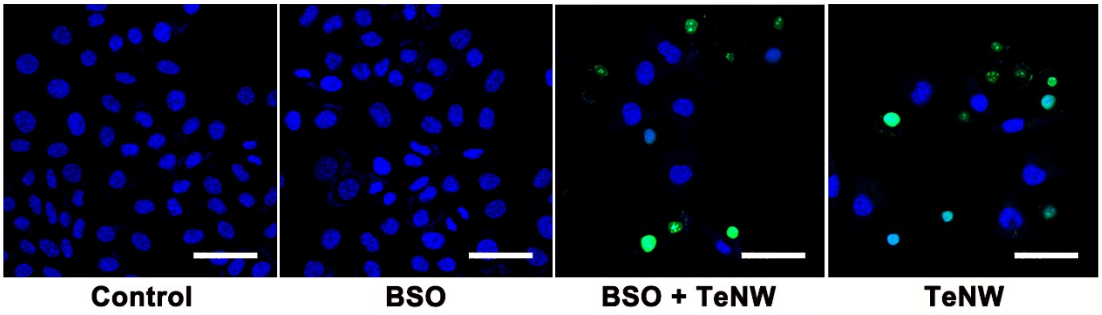

Fig. S15 MCF-7 cells stained with different treatments with TUNEL Assay Kit, in which BSO concentration is 5 μM, and that of TeNW is 32 μg/mL.

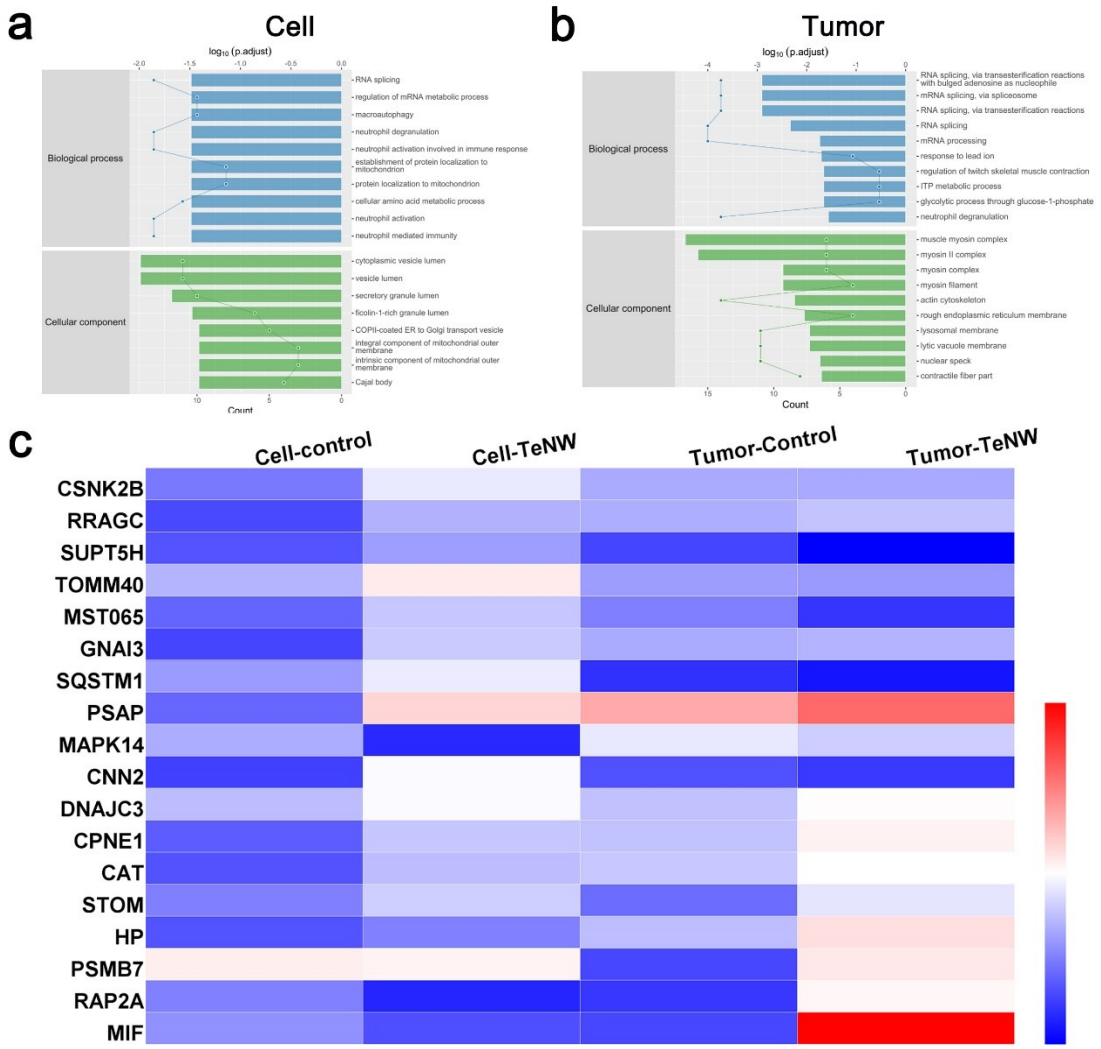

Fig. S16 Enriched GO iterms of MCF-7 cells (a) and tumor treat (b) with TeNW for 24 h, top axis is $\log_{10}$(adjust *p*-value), bottom axis is gene count. (c) Clustering heatmap of relevant significant proteins. ()

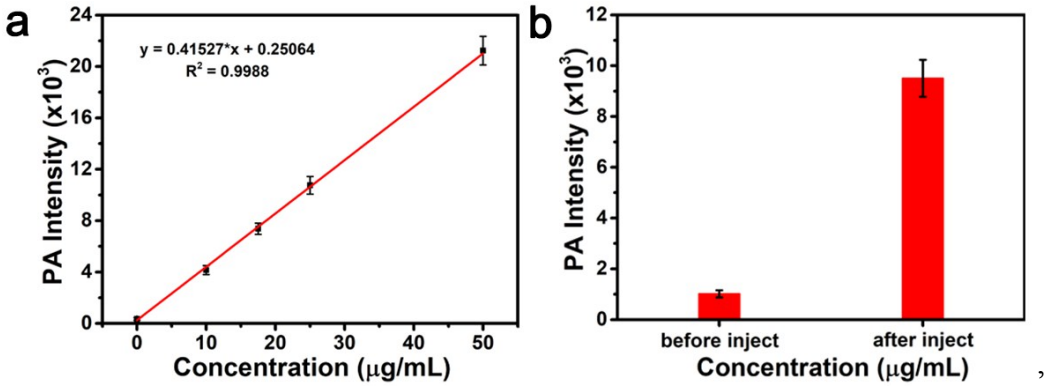

Fig. S17 (a) Corresponding PA intensities of TeNWs solutions with different concentrations. (b) Corresponding quantification of intensities of mice tumor region before and after the injection of TeNWs (0.2 mg kg^{-1}), respectively.

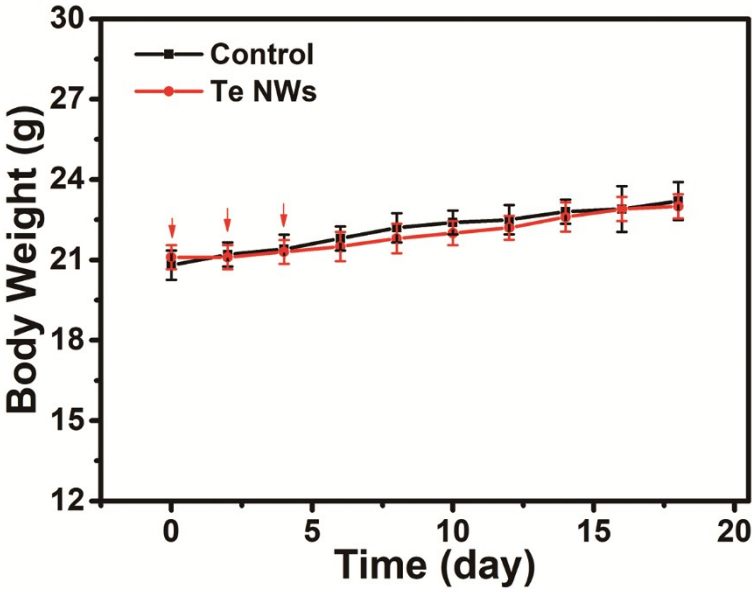

Fig. S18 Time-dependent body-weight curves of nude mice after different treatments as indicated in part.

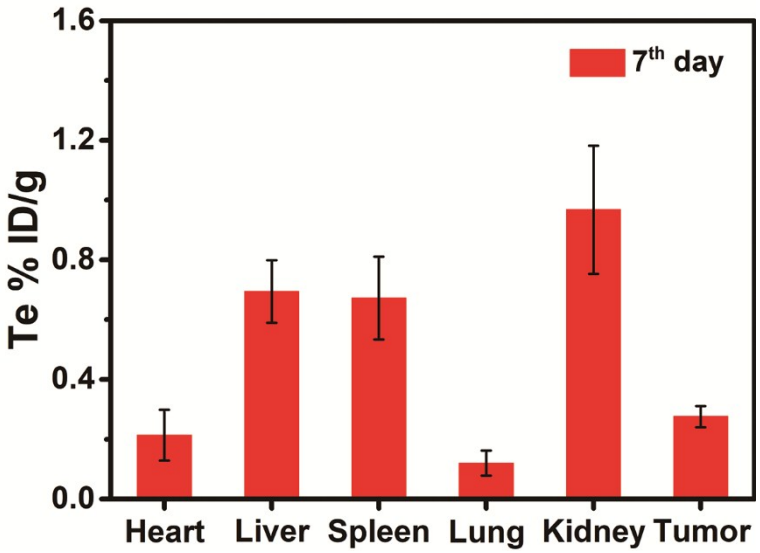

Fig. S19 Long-term biodistribution of Te after the intravenous administration of TeNWs into MCF-7 tumor-bearing mice on 7th day.

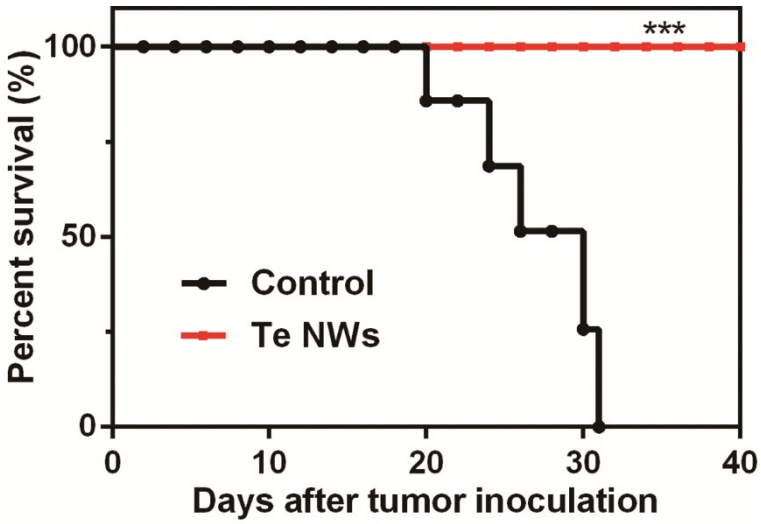

Fig. S20 Survival curves of mice after treated with PBS or TeNW.

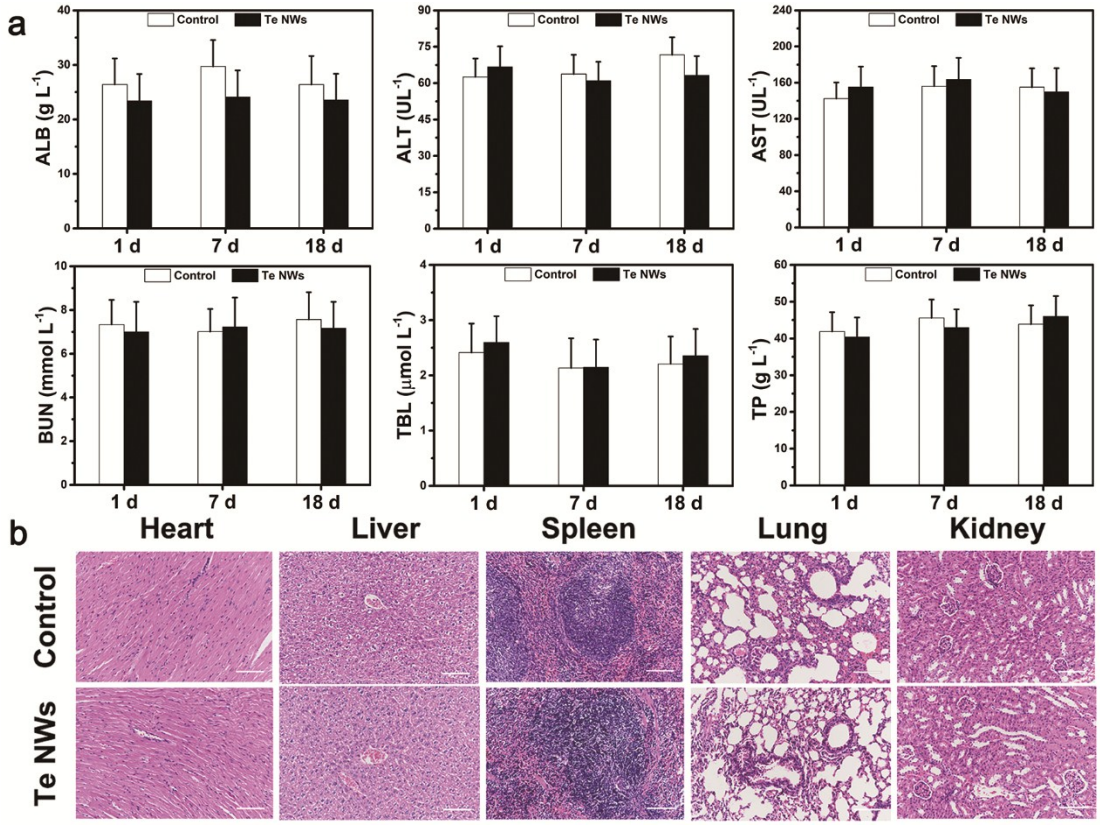

Fig. S21 (a) Biochemical blood analysis of the TeNWs-treated mice 1, 7, and 18 days post-injection under various conditions (control: treat with PBS and TeNWs: treat with TeNWs three times). The terms include ALB, ALT, AST, BUN, TBL, and TP. (b) H&E-stained images of the major organs (heart, liver, spleen, lung, and kidney) from different groups.